Role of interparticle interactions on the magnetic behavior of $Mg_{0.95}Mn_{0.05}Fe_2O_4$ ferrite nanoparticles

2008 J. Phys.: Condens. Matter 20 235214

(http://iopscience.iop.org/0953-8984/20/23/235214)

J. Phys.: Condens. Matter **20** (2008) 235214 (8pp) doi:10.1088/0953-8984/20/23/235214

Role of interparticle interactions on the magnetic behavior of $Mg_{0.95}Mn_{0.05}Fe_2O_4$ ferrite nanoparticles

S K Sharma[1,7], Ravi Kumar[2], Shalendra Kumar[3], M Knobel[1], C T Meneses[1], V V Siva Kumar[2], V R Reddy[4], M Singh[5] and C G Lee[6]

[1] Instituto de Fisica Gleb Wataghin, Universidade Estadual de Campinas (UNICAMP) Campinas, 13.083-970, SP, Brazil
[2] Materials Science Division, Inter-University Accelerator Centre, New Delhi, 110 067, India
[3] Department of Applied Physics, Aligarh Muslim University, Aligarh, 202 002, India
[4] UGC-DAE Consortium for Scientific Research, Khandwa Road, University Campus, Indore, 452 017, India
[5] Department of Physics, H P University, Shimla, 171 005, India
[6] School of Nano and Advanced Materials Engineering, Changwon National University, 9 Sarim dong, Changwon-641-773, Republic of Korea

E-mail: surender76@gmail.com

Received 3 December 2007, in final form 4 March 2008
Published 6 May 2008
Online at stacks.iop.org/JPhysCM/20/235214

Abstract

We present here a detailed investigation of the static and dynamic magnetic behavior of a $Mg_{0.95}Mn_{0.05}Fe_2O_4$ spinel ferrite nanoparticle system synthesized by high-energy ball milling of almost identical particle size distributions ($\langle D \rangle = 4.7$, 5.1 and 6.0 ± 0.6 nm). The samples were characterized by using x-ray diffraction, Mössbauer spectroscopy, dc magnetization and frequency dependent real $\chi'(T)$ and imaginary $\chi''(T)$ parts of ac susceptibility measurements. The zero-field-cooled (ZFC) and field-cooled (FC) magnetization have been recorded in a low field and show a behavior typical of superparamagnetic particles above a temperature of 185 ± 5 K, which is further supported from the temperature dependent Mössbauer measurements. The fact that the blocking temperature calculated from the ZFC magnetization and Mössbauer data are almost similar gives a clear indication of the interparticle interactions among these nanoparticle systems. This is further supported from the FC magnetization curves, which are almost flat below a certain temperature (less than the blocking temperature), as compared with the monotonically increasing behavior characteristics of non-interacting superparamagnetic particles. A shift of the blocking temperature with increasing frequency was observed in the real $\chi'(T)$ and imaginary $\chi''(T)$ parts of the ac susceptibility measurements. The analysis of the results shows that the data fit well with the Vogel–Fulcher law, whereas trials using the Neel–Brown and power law are unproductive. The role of magnetic interparticle interactions on the magnetic behavior, namely superparamagnetic relaxation time and magnetic anisotropy, are discussed.

1. Introduction

Nanocrystalline ferrite materials display a variety of remarkable and fascinating magnetic properties when compared to their bulk counterparts. Owing to strong modifications in surface/interface effects, electronic states and magnetic interactions in the nanometer range, the nanocrystalline ferrites exhibit some diverse features such as an enhanced/reduced saturation magnetization, low/high coercivity, superparamagnetic (SPM) relaxation, spin-glass-like (SG) behavior, spin canting and a B–H loop shift as compared to bulk ferrites [1–4]. Below some critical dimension, magnetic particles become single-

[7] Author to whom any correspondence should be addressed.

domain and show superparamagnetic (SPM) behavior [5–7]. Because of such a wide range of features, magnetic nanoparticles have been routinely applied in magnetic recording media, ferrofluids and catalysis [1–4]. The magnetic properties of such particles are well described by the Neel–Brown model [8], where the magnetic anisotropy energy E_A is a major factor in determining the magnetic behavior of nanoparticles. Above the blocking temperature T_B, the thermal energy k_BT and applied field shift the magnetization direction of the nanoparticles away from their easy axis and particles shows superparamagnetism (SPM). In the Neel–Brown model, the particles are considered to be non-interacting. Conversely, when the interparticle interactions are strong enough, a magnetic phase transition from superparamagnetic (SPM) to a collective spin-glass (SG) state occurs [9]. However, in real nanostructured systems, the magnetic properties are governed by both the intrinsic magnetic anisotropy energy and interparticle interactions. Further, the interactions between superparamagnetic (SPM) nanoparticles have been taken into account in the Vogel–Fulcher [10] model, a modified form of the Neel–Brown model. In addition, a power law, which assumes the existence of a true equilibrium phase transition with a discrepancy of the relaxation time near the transition temperature, has been used to explain the relaxation mechanism involved in spin-glass (SG) and cluster-spin-glass systems [11–14]. These three models have been successfully applied to explain the magnetic properties of different superparamagnetic and spin-glass systems in the literature [15–18].

Among the variety of preparation techniques of ferrites nanoparticles, ball milling has been recognized as one of the most potential for the production of large amounts of nanoparticle material. Zhou *et al* [19] has observed a rich variety of non-equilibrium magnetic states, such as superparamagnetic (SPM) or spin-glass etc [20, 21], in ball milled nanoparticles of Co_2Ge alloy and thus it has become very important to study non-equilibrium spin.

In this paper, we have investigated the role of interparticle interactions on the static and dynamic behavior of $Mg_{0.95}Mn_{0.05}Fe_2O_4$ ferrite nanoparticles of almost identical particle size distribution prepared by ball milling.

2. Experimental details

Bulk particles of $Mg_{0.95}Mn_{0.05}Fe_2O_4$ were synthesized using a standard solid-state reaction technique. A stoichiometric amount of MgO, MnO and Fe_2O_3 were mixed thoroughly and pre-heated at 1000 °C for 12 h for calcination. The calcinated powder was pressed into pellets and sintered at 1300 °C for 24 h, followed by slow cooling to room temperature. To prepare the nanoparticles, 5 g of the resulting material was milled in a high-energy ball mill (SPEX 8000D). Two hardened stainless steel vials (72 cm^3) charged with five hardened steel balls of 12 mm diameter and three of 6 mm diameters were used for the milling. The ball to powder mass ratio was fixed at 10:1. The powder was milled in air at room temperature without any additives under closed conditions for varying times namely, 8, 10 and 12 h. These samples will henceforth be labeled as SX, where each X number refers to the total hours of milling time. To understand the structure and particle sizes, powder x-ray diffraction measurements were performed using a Siemens x-ray diffractometer (D5000). The Mössbauer spectroscopy measurements were performed using a conventional constant acceleration spectrometer in transmission geometry with a ^{57}Co source in a Rh matrix in the temperature range 20–300 K. The Mössbauer spectra were analyzed with the standard least squares fitting program NORMOS (SITE) [22]. Lorentzian lines shapes were used to fit the recorded Mössbauer spectra. All the isomer shifts are given relative to that of α-Fe at room temperature. The dc magnetization measurements were done using a Quantum Design MPMS XL7 SQUID magnetometer in both zero-field-cooled (ZFC) and field-cooled (FC) modes in the range 5 K $\leqslant T \leqslant$ 300 K in the presence of a low magnetic field of 20 Oe. The real and imaginary parts of the ac magnetic susceptibility were measured at frequencies in the range 31 Hz $\leqslant f \leqslant$ 1131 Hz with a field amplitude of 2 Oe on a home-made susceptometer [23] in the temperature range 80–300 K.

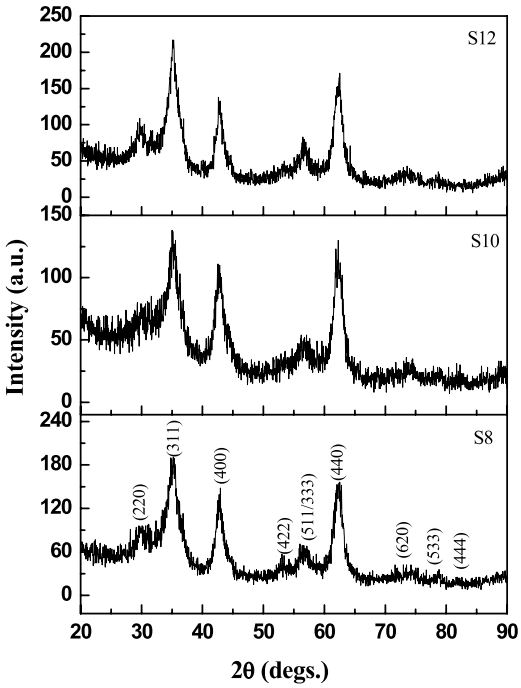

Figure 1. X-ray diffraction pattern for samples S8, S10 and S12. The Miller indices (hkl) for the major peaks are also shown.

3. Results and discussion

3.1. X-ray diffraction

Figure 1 shows the x-ray diffraction patterns for samples S8, S10 and S12 and exhibit several reflections corresponding to the characteristic interplane spacings (220), (311), (400), (422), (333/511), (440), (620), (533) and (444), which confirms the formation of a single-phase cubic spinel structure with no extra phase. From the XRD patterns, it is clearly evident that the reflection lines are quite broad, suggesting the powder crystallites have been reduced into nanosized particles. The maximum intensity peak (311) was fitted with a Gaussian shape to calculate the exact peak position and

Table 1. Some properties of nanoparticle samples S8, S10 and S12: ball milling time, average particle size $\langle D \rangle$ (from x-ray line broadening), blocking temperature T_B calculated from dc magnetization and Mössbauer data, relative shift in the real part $\chi'(T)$ of the ac susceptibility Φ and hyperfine parameters at 20 and 300 K: isomer shift (IS), quadrupolar splitting (QS), hyperfine field (B_{hyp}).

Sample	Time (h)	D (nm) ($\pm$ 0.6)	dcT_B (K) ($\pm$ 5)	T_{BM} (K) ($\pm$ 5)	Φ	T (K)	Sites	IS (mm s^{-1}) ($\pm$ 0.01)	QS (mm s^{-1}) ($\pm$ 0.01)	B_{hyp} (kOe) ($\pm$ 2)
S8	8	5.1	232	236	0.06	20	A	0.19	−0.0658	474.41
							B	0.28	−0.0010	516.45
						300	Sextet	0.38	0.871	400.73
							Doublet	0.32	0.114	—
S10	10	4.7	188	192	0.03	20	A	0.24	−0.0918	486.74
							B	0.30	−0.0109	519.78
						300	Sextet	0.16	−0.279	339.14
							Doublet	0.33	0.819	—
S12	12	6.0	195	198	0.01	20	A	0.42	−0.0463	513.36
							B	0.45	−0.0246	549.86
						300	Doublet	0.27	1.247	—
							Doublet	0.32	0.810	—

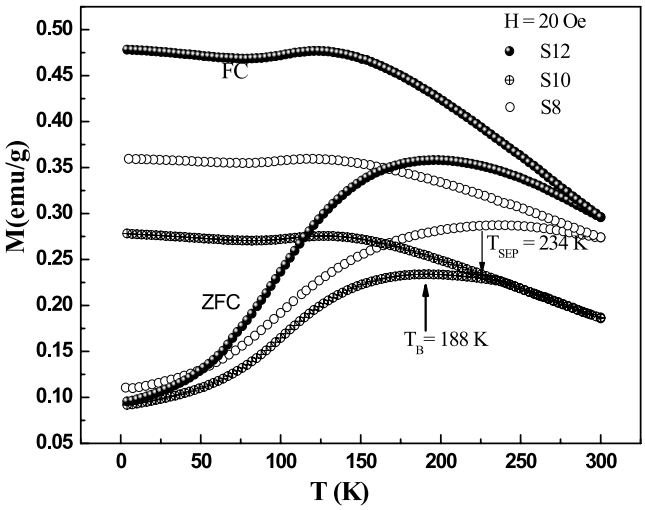

Figure 2. Zero-field-cooled (ZFC) and field-cooled (FC) curves for samples S8, S10 and S12 taken in an external field of $H = 20$ Oe.

the full width half maximum (FWHM). The average particle size was calculated from the (311) peak without considering the possible contributions of crystal strain to the observed broadening by using Scherrer's equation [24];

$$D = \frac{k\lambda}{B\cos\theta} \tag{1}$$

where D is the average particle size, k is a shape factor (assumed to be 0.9) and λ is the wavelength of the incident x-rays. Here $B = (B_M^2 - B_S^2)^{1/2}$, where B_M is the full width at half maximum (FWHM) of the (311) peak and B_S is the standard instrumental broadening. The average particle sizes calculated using equation (1) are given in table 1 and consist of nanosized particles for which superparamagnetic effects should be expected.

3.2. Magnetization data

To further study these nanoparticles, we have performed magnetization measurements as functions of both temperature and applied field. Figure 2 shows the variation of magnetization M as function of temperature (T) in the range 5–300 K in an external magnetic field of 20 Oe recorded in zero-field-cooled (ZFC) and field-cooled (FC) modes for the samples S8, S10 and S12. In the ZFC mode, the sample was cooled in zero field from 300 to 5 K and after stabilization of the temperature, a measuring field of 20 Oe was applied. The data were then recorded whilst warming the sample. In the FC mode, the sample was cooled down from 300 to 5 K in the presence of a field of 20 Oe and then measurements were carried out whilst warming in the same field. From the curves, it is clearly seen that bifurcation of the ZFC and FC curves at a certain temperature T_{SEP} (figure 2) is one of the characteristic features of a superparamagnetic (SPM) system. However, the coinciding broad maximum are observed in the ZFC curves at a slightly lower temperature (denoted as T_B here) than T_{SEP}. Such a behavior usually indicates a certain particle size distribution in the nanoparticle system, where a fraction of the largest particles has already frozen at T_{SEP} with the majority fraction of the nanoparticles being blocked at T_B, resulting in a distribution of the blocking temperatures in the samples. The maxima of the ZFC curve is located at $T_B = 232$, 188 and 195 K (with an uncertainty of $\pm$5 K) for samples S8, S10 and S12 respectively. In addition, M_{ZFC} strongly decreases below T_B, since the change from the superparamagnet to ferromagnetic regime initiates the anisotropy, forcing the magnetization along the easy axes, are randomly oriented. This decrease in M_{ZFC} is also observed above T_B, as we approach the superparamagnetic (SPM) regime. From these curves, a clear thermo-magnetic irreversibility can be easily seen from the distinct difference between M_{ZFC} (T) and M_{FC} (T) below a certain temperature T_{SEP}. Both the ZFC and FC curves tended to be superimposed above T_{SEP} (296 $\pm$ 5 K, 234 $\pm$ 5 K, 275 $\pm$ 5 K) as the superparamagnetic (SPM) state was reached for samples S8, S10 and S12 respectively. In fact, such behavior is characteristic of superparamagnetism (SPM) and a spin-glass (SG)-like state [25]. In addition, the M_{FC} values are almost constant below a certain temperature (less than T_B), and this constant value is much higher than that of the M_{ZFC} values. The fact that the field-cooled (FC) curve was nearly flat below T_B, as compared

with the monotonically increasing behavior characteristic of non-interacting or superparamagnetic systems, indicated the existence of strong interactions among these nanoparticle systems [25]. However, this feature has been recently found not only to be exclusive of SG, but also shared by other nanoparticle systems having a random anisotropy and strong interparticle interactions [26, 27]. In the present case a broad peak in the FC curve at low fields with a small decline in magnetization below T_B is observed, suggesting the existence of strong interactions in our system in agreement with previously published results in the literature [28, 29]. The effects of these interactions was also investigated by means of an ordering temperature T_0 calculated from the high temperature superparamagnetic (SPM) regime. In the case of non-interacting superparamagnetic (SPM) particles, it was expected that in this region the system would obey the Curie law $\chi = C/T$. For an assembly of interacting superparamagnetic (SPM) particles, the low field susceptibility is expected to be of the form,

$$\chi \sim \frac{\mu_{\text{mean}}}{3k_B\,(T - T_0)} \tag{2}$$

where μ_{mean} is the mean magnetic moment per particle, k_B is the Boltzmann constant and T_0 is the effective temperature arising from the interparticle interactions. According to equation (2), the inverse of the field-cooled (FC) susceptibility should be linear above T_B. We observed that the linear law was only obeyed for $T > 259$ K (the figure not shown here) and the extrapolated value of T $_0$ for all the investigated samples was 193 ± 3 K. These facts further supported the existence of strong interparticle interactions with a magnetizing character.

3.3. Mössbauer measurements

^{57}Fe Mössbauer spectroscopy is a powerful tool to characterize ferrite nanoparticles undergoing superparamagnetic (SPM) relaxation. Figures 3(a)–(c) show the Mössbauer spectra recorded for all the investigated samples (in the temperature range 20–300 K). The dots in figure 3 represent the experimental data and the solid lines through data points are least squares fittings. The other solid lines within each spectrum indicate the positions of the tetrahedral (A-site) and octahedral (B-site) resonance lines. In fact, all the samples show a typical superparamagnetic (SPM) behavior, i.e., the spectra are dominated by sextets at low temperatures, but with increasing temperature a central doublet becomes increasingly dominant, which is asymmetric due to superparamagnetic (SPM) relaxation effects. In the SPM state, the magnetic hyperfine interactions are averaged to zero, due to fast relaxation of particle magnetic moments, so that the resulting Mössbauer spectra consist of a paramagnetic-like doublet. However, due to a distribution of energy barriers, some nanoparticles relax faster and others slower at a given temperature. Consequently, the sextet peak and the doublet peak can appear simultaneously. The sextet peak represents the fraction of nanoparticles with relaxation time longer than the Mössbauer measurements time 10^{-9} s, whereas the doublet peak represents the fraction of nanoparticles with relaxation time shorter than 10^{-9} s. From the analysis of Mössbauer spectra, we have calculated the relative areas of the doublets and sextets. Using a linear extrapolation of these areas as a function of temperature, we define the blocking temperature T_B, as the temperature where the sextet collapses to 50 % of its initial value. From the extrapolation, we found that for the S8 sample, T_B is around 236 ± 5 K and decreases with a decrease in the particle size. The corresponding values of the blocking temperatures along with the hyperfine parameters at 20 and 300 K are shown in table 1. It is interesting to see that the blocking temperature T_B calculated from Mössbauer and dc magnetization data are found to have almost identical values within the experimental error. In general, the T_B determined by Mössbauer spectroscopy is higher than that determined by SQUID magnetometry and this can be explained by Neel–Brown theory. However, the similar values found in the present study further support the occurrence of interparticle interactions among these nanoparticle samples.

3.4. Susceptibility measurements

In order to further authenticate and get a better insight into the nature of these interparticle interactions, we also investigated the temperature dependence of the real and imaginary parts, $\chi'(T)$ and $\chi''(T)$, of ac susceptibility measurements for different driving frequencies in the range from 31 to 1131 Hz (see figures 4(a) and (b)) for samples S10 and S12. It is clearly evident from figure 4 that the data for both $\chi'(T)$ and $\chi''(T)$ exhibit the expected behavior of a blocking/freezing process, i.e. the occurrence of a maximum at a temperature T_B for both $\chi'(T)$ and $\chi''(T)$ components which shifts towards higher temperature and decreases in height with increasing frequency [30]. In order to identify the dynamic behavior of the blocking/freezing process, we have used the real part $\chi'(T)$ of ac susceptibility in an empirical relation,

$$\Phi = \frac{\Delta T_B}{T_B \Delta \log_{10}(f)} \tag{3}$$

here ΔT_B is the difference between the T_B measured in the $\Delta \log_{10}(f)$ frequency interval and f is the ac magnetic field frequency. In fact, this parameter provides a model-independent classification of the blocking/freezing process. The experimentally found values for the superparamagnetic (SPM) particles are in the range ∼0.1–0.13, whereas a much smaller value was found in the present case (see table 1) usually observed for spin-glass (∼0.005–0.05) behavior of the nanoparticle surface or simply due to non-negligible interparticle interactions [31]. In fact, it is well known that smaller values of Φ usually result from strong interactions and the spin-glass hypothesis [30, 32, 33]. However, it is often very difficult to distinguish between SG and SPM experimentally [34]. There are two different main interpretations in the literature on the phenomenon of the spin-glass freezing. For a system consisting of non-interacting superparamagnetic particles, the relaxation time τ follows the Neel–Arrhenius (NA) relation,

$$\tau = \tau_o \exp\left(\frac{E_A}{k_B T_B}\right), \tag{4}$$

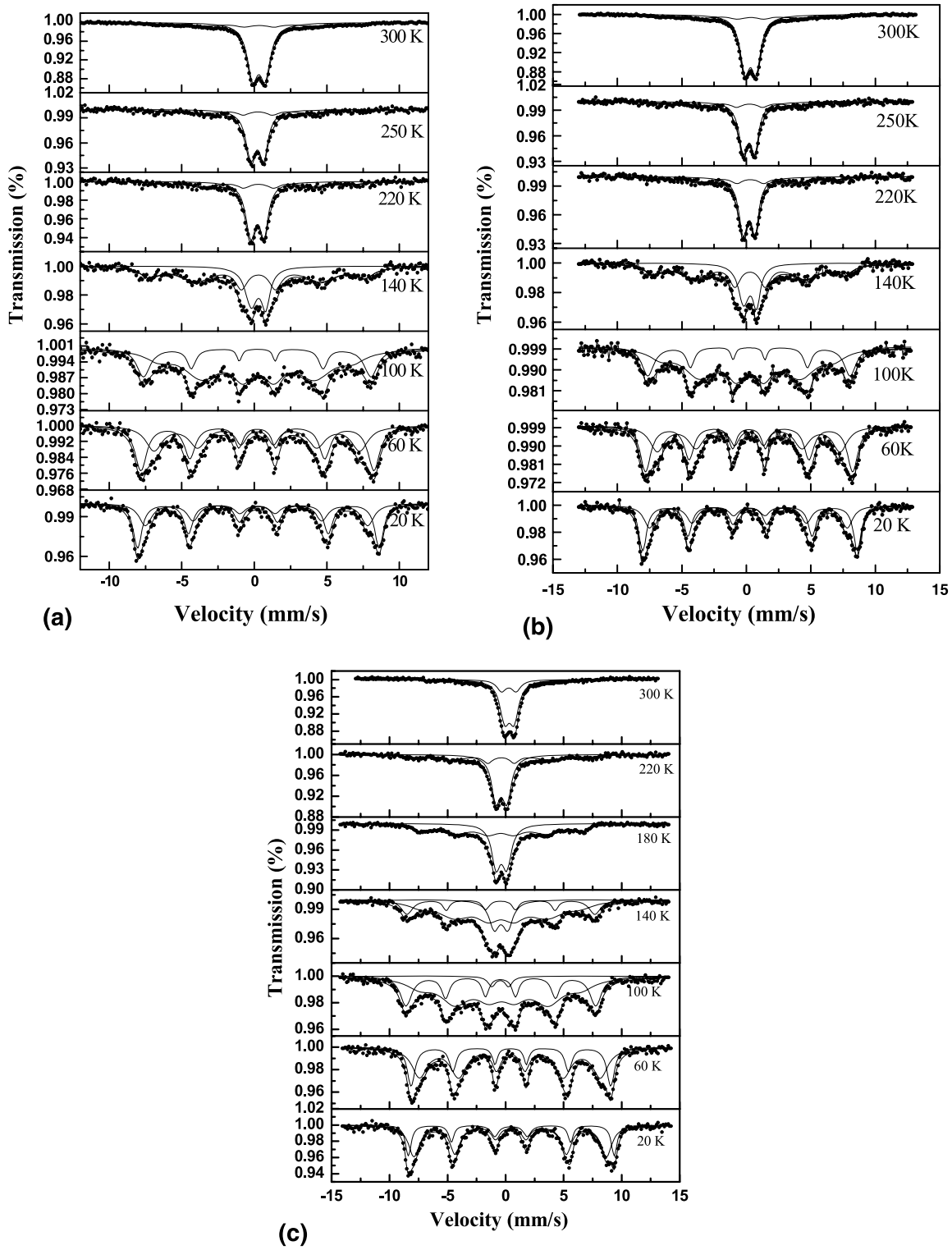

Figure 3. Mössbauer spectra of sample (a) S8, (b) S10 and (c) S12 in the temperature range from 20 to 300 K.

where τ is the relaxation time at frequency f, E_A is the anisotropy energy barrier for the reversal of the moments and τ_0 is the characteristic relaxation time, ranging typically from 10^{-9} to 10^{-13} s for superparamagnetic (SPM) particles. In an external magnetic field, the energy barrier is given by $E_A = K_{eff}V$, where K_{eff} is an effective magnetic anisotropy constant and V is the particle volume. To confirm the validity of the Neel–Arrhenius (NA) relation, we first plot $\ln\tau$ versus $1/T_B$ for both systems (for brevity this is not shown here). From the fitting, we have found an unphysically small value of relaxation time; $\tau_0 \sim 1.1 \times 10^{-16}$ for S10 and 6×10^{-69} s for S12 in comparison to 10^{-13} s. This leads us to conclude that the Neel–Arrhenius (NA) relation is not valid and there exist strong interactions among these nanoparticle systems [34],

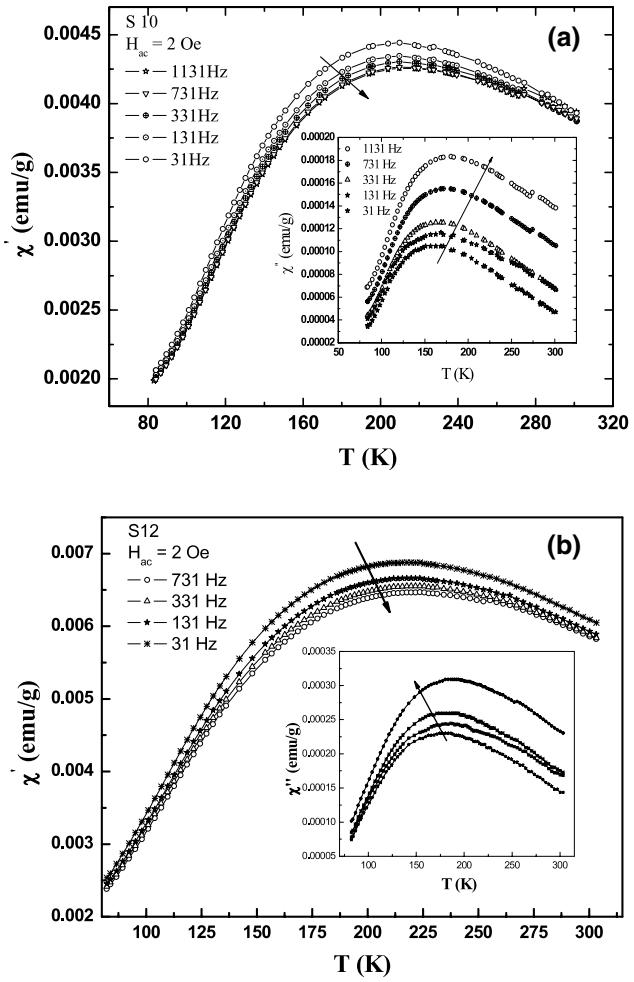

Figure 4. Temperature dependence of the real part $\chi'(T)$ of the ac magnetic susceptibility for the (a) S10 and (b) S12 samples, at different frequencies. The arrow indicates increasing frequencies. Inset: imaginary part $\chi''(T)$. The data were taken with an external magnetic field, $H = 2$ Oe.

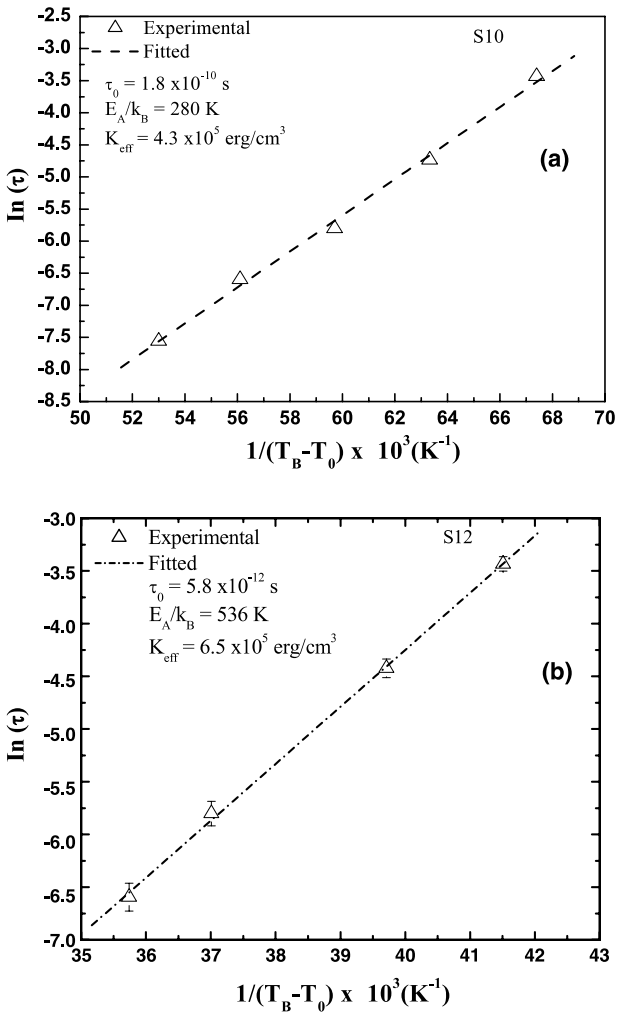

Figure 5. Logarithm of the measuring frequency as a function of the reciprocal of the difference between the temperature of peak and T_0 for samples (a) S10 and (b) S12.

consistent with the results obtained from the dc magnetization and Mössbauer data. As a result, we have tried to fit these data using the Vogel–Fulcher (VG) law [10], that describes the slowing down of a system composed of magnetically interacting particles as the temperature is reduced, and can be expressed in the form

$$\tau = \tau_o \exp\left(\frac{E_A}{k_B\,(T_B - T_0)}\right). \qquad (5)$$

Here T_0 is an effective temperature with a similar origin to that used to reproduce the dc susceptibility in the superparamagnetic regime and T_B is the characteristic temperature signaling the onset of the blocking process (i.e. the temperature of the peak position in the ac susceptibility). In this case, the experimental data can be fitted to the equation (5) as shown in figures 5(a) and (b) for samples S10 and S12 respectively, giving the following values of the parameters: $\tau_0 = 1.8 \times 10^{-10}$ s, $E_A = 3.8 \times 10^{-18}$ erg, $T_0 = 195$ K and $\tau_0 = 5.8 \times 10^{-12}$ s, $E_A = 7.4 \times 10^{-17}$ erg and $T_0 = 195$ K. A good agreement between the experimental data and the Vogel–Fulcher (VG) law indicates that the phenomenon taking place at the maximum of susceptibility curve is related to blocking of an assembly of interacting particles rather that a collective freezing (as occurs in a spin-glass system). This is further confirmed from the power law discussed below. The large value observed in the present case is expected from strong interparticles interactions, but the experimentally determined value τ_0 for the sample S12 is much lower than that of S10. This may possibly be due to the fact that interactions are more relevant for the S12 sample than for the S10 sample. By fitting the experimental data with equation (5) and using the average particle size calculated from XRD data, the calculated values of K_{eff} for sample S10 and S12 are 4.5×10^5 and 6.5×10^5 erg cm^{-3} respectively. The resulting effective anisotropy is larger than that of magnetocrystalline anisotropy constant of bulk ferrite [35], which is an expected behavior of nanosized particles, where the surface contribution is expected to enhance the magnetic anisotropy constant.

Further, we have also checked the existence of spin-glass (SG) behavior through a conventional critical slowing down model [36–38], which states that close to the spin-glass transition, the characteristic relaxation time ($\tau = 1/f$) of

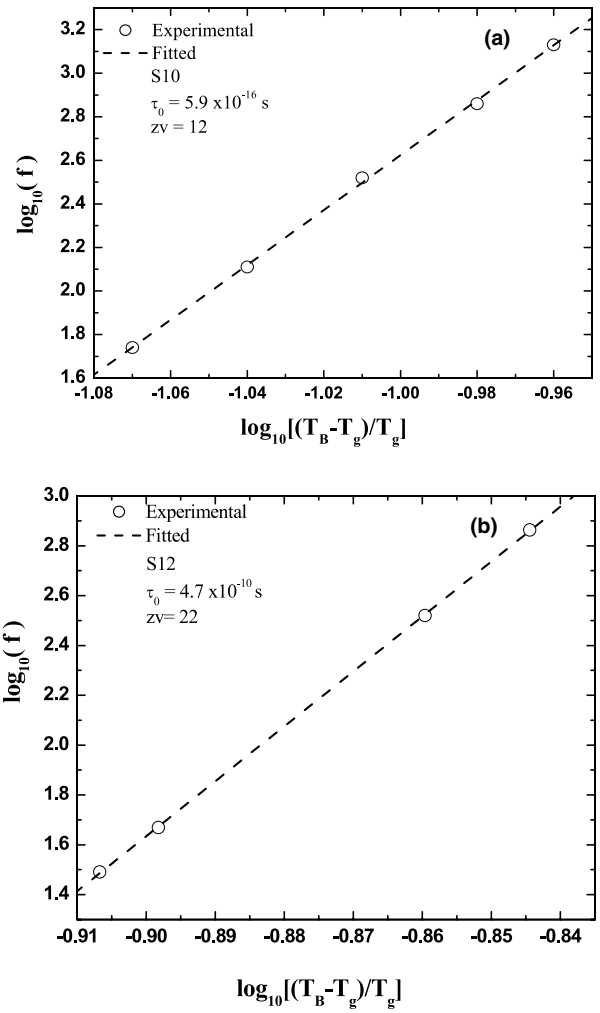

Figure 6. A log–log plot of the reduced temperature $\varepsilon = (T_B - T_g)/T_g$ versus frequencies for sample (a) S10 and (b) S12.

the individual magnetic moments will show a slowing down obeying a conventional power law,

$$\tau = \tau_0 \varepsilon^{-zv} \tag{6}$$

where $\varepsilon = (T_B - T_g)/T_g$ denotes a reduced temperature, τ_0 is the microscopic relaxation time, z is the dynamical scaling exponent, T_g is the spin-glass freezing temperature and v is the correlation length scaling exponent. Hence, the frequency (f) dependent maxima should follow the relation,

$$f = f_0 \varepsilon^{zv}. \tag{7}$$

A log–log plot of the reduced temperature $(T_B - T_g)/T_g$ versus external frequencies (f) gives an excellent linear dependence as shown in figures 6(a) and (b) for sample S10 and S12 respectively. The best fitting parameters are; $\tau_0 = 5.9 \times 10^{-16}$ s, $zv = 12 \pm 3$, $T_g = 193 \pm 3$ K for sample S10, whereas for sample S12 $\tau_0 = 4.7 \times 10^{-10}$ s, $zv = 20 \pm 3$, $T_g = 193 \pm 3$ K. The estimated values of critical exponents zv and τ_0 are not consistent with the values obtained for spin-glass systems, but are also different from those extracted using the Vogel–Fulcher law. For spin-glasses, typical values of τ_0 are within the range 10^{-11}–10^{-12} s [38]. This further strengthens our result that a blocking of the interacting particles occurs rather than the collective nature of a spin-disordered system, such as a spin-glass. On the other hand, parameters that we obtained by using the Vogel–Fulcher law have reasonable values. This would imply that a factual SG transition does not exist in these nanoparticle systems.

4. Conclusion

In conclusion, we have studied the role of interactions on the static and dynamic properties of $Mg_{0.95}Mn_{0.05}Fe_2O_4$ ferrite nanoparticles having almost identical size distribution using x-ray diffraction, Mössbauer spectroscopy, dc magnetization and ac susceptibility measurements. DC magnetization and Mössbauer studies show the onset of blocking of particles above a certain temperature of 185 ± 5 K for all the investigated samples. The T_B calculated from the ZFC magnetization and the Mössbauer data are found to have almost identical values giving a clear indication of the role of that interparticle interactions play in these nanoparticle systems. This is further supported by the FC magnetization. The dynamic behavior of these nanoparticles is strongly influenced by interparticle interactions which are present in all the samples and are well described by the Vogel–Fulcher (VG) law for interacting superparamagnetic (SPM) particles. On the other hand, attempts to fit the data with a Neel–Brown (NA) model for thermally non-interacting superparamagnetic (SPM) particles and a power law for spin-glasses is unsuccessful and both yield an unphysically small value of the relaxation time constant τ_0.

Acknowledgments

Authors (SKS and MK) are very grateful to FAPESP and CNPq (Brazil) for providing financial support.

References

[1] Ding J, Reynold T, Miao W F, McCormick P G and Street R 1994 *Appl. Phys. Lett.* **65** 7074
[2] Kodama R H, Berkowitz A E, McNiff E J and Foner S 1966 *Phys. Rev. Lett.* **77** 395
[3] Ding J, Miao W F, Street R and McCormick P G 1988 *J. Alloys Compounds* **281** 32
[4] Martinez B, Obradors T, Balcell L I, Rounanet A and Monty C 1998 *Phys. Rev. Lett.* **80** 181
[5] Kodama R H, Berkowitz A E, McNiff E J and Foner S 1996 *Phys. Rev. Lett.* **77** 394
[6] Kodama R H 1999 *J. Magn. Magn. Mater.* **200** 359
[7] Tronc E, Fiorani D, Noguès M, Testa A M, Lucari F, D'Orazio F, Grenèche J M, Wernsdorfer W, Galvez N and Chanéac C 2003 *J. Magn. Magn. Mater.* **262** 69
[8] Neel L 1949 *Ann. Geophys.* **5** 99
[9] Sahoo S, Petracic O, Binek Ch, Kleemann W, Sousa J B, Cardoso S and Freitas P P 2002 *J. Phys.: Condens. Matter* **14** 6729
[10] Shtrikman S and Wohlfarth E P 1981 *Phys. Lett.* A **85** 467
[11] Ogielski A T 1985 *Phys. Rev.* B **32** 7384
[12] Martinez B, Labarta A, Rodriguez-Sola R and Obradors X 1994 *Phys. Rev.* B **50** 15779
[13] Souletie J and Tholence J L 1985 *Phys. Rev.* B **32** R516

[14] Hohenberg P C and Halperin B I 1977 *Rev. Mod. Phys.* **49** 435
[15] Tholence J L 1980 *Solid State Commun.* **35** 113
[16] Tholence J L 1981 *Physica* B+C **108** 1287
[17] Tholence J L 1979 *J. Appl. Phys.* **50** 7310
[18] Cardoso C A, Araujo-Moreira F M, Awana V P S, Takayama-Muromachi E, De Lima O F, Yamauch H and Karppinen M 2003 *Phys. Rev.* B **67** 020407 (R)
[19] Zhou G F and Bakker H 1994 *Phys. Rev. Lett.* **72** 2290
[20] De Toro J A, Lopez de la Torre M A, Riveiro J M, Sacz Puche R, Gomez-Herrero A and Otero-Diaz L C 1999 *Phys. Rev.* B **60** 12918
[21] De Toro J A, Lopez de la Torre M A, Riveiro J M, Bland J, Goff J P and Thomas M F 2001 *Phys. Rev.* B **64** 224421
[22] Brand R A, Lauer J and Herlach D M 1984 *J. Phys. F: Met. Phys.* **14** 55
[23] Bajpaians A and Banerjee A 1999 *Rev. Sci. Instum.* **68** 4075
[24] Cullity B D 1987 *Elements of X-ray Diffraction* (Reading, MA: Addison-Wesely)
[25] Bitoh T, Ohba K, Takamatsu M, Shirane T and Hikazawa S 1995 *J. Phys. Soc. Japan* **64** 1305
[26] Mamiya H, Nakatani I and Furubayashi T 1998 *Phys. Rev. Lett.* **80** 177
[27] Battle X, Garcia del Muro M and Labarta A 1997 *Phys. Rev.* B **55** 6440
[28] Tung L D, Kolesnichenko V, Caruntu G, Caruntu D, Remond Y, Golub V O, O'Connor C J and Spiny L 2002 *Physica* B **319** 116
[29] Fonseca F C, Goya G F, Jardim R F, Muccilo R, Carreño N L V, Longo E and Leite E R 2002 *Phys. Rev.* B **6** 104406
[30] Dormann J L, Fiorani D and Tronc E 1997 *Adv. Chem. Phys.* **98** 326
[31] Goya G F and Sagredo V 2001 *Phys. Rev.* B **64** 235
[32] Goya G F 2002 *IEEE Trans. Magn.* **38** 2610
[33] De Toro J A, Lopez de la Torre M A, Arranz M A, Riveiro J M, Marinez J L, Palade P and Filoti G 2001 *Phys. Rev.* B **64** 094438
[34] Mydosh A 1993 *Spin Glasses: An Experimental Introduction* (London: Taylor and Francis)
[35] Cullity B D 1972 *Introduction to Magnetic Materials* (Reading, MA: Addison-Wesely)
[36] Souletie J and Tholence J L 1985 *Phys. Rev.* B **32** R516
[37] Ogielski A T 1985 *Phys. Rev.* B **32** 7384
[38] Idzikowski B, Robler U K, Eckert D, Nenkov K, Dorr K and Muller K H 1999 *Europhys. Lett.* **45** 714